

# Infrared and optical properties of pure and cobalt-doped $\text{LuNi}_2\text{B}_2\text{C}$ .

M. Windt,\* J. J. McGuire, T. R  m,† A. Pronin,‡ and T. Timusk§

*Department of Physics and Astronomy, McMaster University, Hamilton ON Canada, L8S 4M1*

I.R. Fisher and P.C. Canfield

*Ames Laboratory, Department of Physics and Astronomy, Iowa State University, Ames, Iowa 50011*

We present optical conductivity data for  $\text{Lu}(\text{Ni}_{1-x}\text{Co}_x)_2\text{B}_2\text{C}$  over a wide range of frequencies and temperatures for  $x=0$  and  $x=0.09$ . Both materials show evidence of being good Drude metals with the infrared data in reasonable agreement with dc resistivity measurements at low frequencies. An absorption threshold is seen at approximately  $700\text{ cm}^{-1}$ . In the cobalt-doped material we see a superconducting gap in the conductivity spectrum with an absorption onset at  $24 \pm 2\text{ cm}^{-1} = 3.9 \pm 0.4k_B T_c$  suggestive of weak to moderately strong coupling. The pure material is in the clean limit and no gap can be seen. We discuss the data in terms of the electron-phonon interaction and find that it can be fit below  $600\text{ cm}^{-1}$  with a plasma frequency of  $3.3\text{ eV}$  and an electron-phonon coupling constant  $\lambda_{tr} = 0.33$  using an  $\alpha^2 F(\omega)$  spectrum fit to the resistivity.

PACS numbers: 74.70.Dd, 78.20.Ci, 78.30.Er

## I. INTRODUCTION

The recent discovery of superconductivity at  $39\text{ K}$  in  $\text{MgB}_2$  has renewed interest in intermetallic superconductors containing boron. There have been suggestions that their high transition temperatures may result from an exotic mechanism and not from a conventional s-wave BCS phonon process. The borocarbide family of superconductors  $\text{LNi}_2\text{B}_2\text{C}$ , where  $L=(\text{Y},\text{Lu},\text{Tm},\text{Er},\text{Ho},\text{and Dy})$  shows a number of physical properties that suggest that they may be a testing ground for these ideas.<sup>1</sup> For example, recent measurements of heat capacity and microwave surface impedance in the vortex state suggest that low energy quasiparticles may have d-wave dispersion.<sup>2,3</sup> The critical field temperature variation has an upward curvature that is difficult to explain within the BCS theory.<sup>2,4</sup> Other suggestions of abnormal behavior include residual absorption in the gap seen by Raman spectroscopy<sup>5,6</sup> and the sensitivity of the transition temperature to non-magnetic impurities.<sup>7,8</sup> On the other hand, there is a lot of the evidence that supports a conventional s-wave mechanism of superconductivity for these materials. This includes good agreement between transport and critical field properties based on Eliashberg theory<sup>9,10</sup> and s-wave-like tunneling spectra.<sup>11</sup>

Within the s-wave, electron-phonon picture, there are two routes to high transition temperatures: a large coupling constant  $\lambda$  or the coupling to very high frequency modes with modest coupling. It was suggested early on by Pickett *et al.* that unusual electronic structure seen in the borocarbides at the Fermi surface would lead to strong coupling to certain phonons.<sup>12</sup> On the other hand more recent data based on specific heat by Michor *et al.* are consistent with a  $\lambda$  of the order of unity.<sup>13</sup> Gonnelli *et al.* were able to fit the temperature dependence of the dc resistivity of  $\text{YNi}_2\text{B}_2\text{C}$  with a phonon spectrum from inelastic neutron scattering of Gompf *et al.*<sup>15</sup> with a  $\lambda_{tr}$  of only  $0.57$ ,<sup>10</sup> where  $\lambda_{tr}$  is just  $\lambda$  modified by a

factor that depends of the scattering angle.<sup>16</sup> Gompf *et al.* found evidence of soft mode behavior in several modes but not the high frequency mode originally singled out by Mattheiss<sup>17</sup> to couple strongly to the electronic system.

The infrared response of superconductors can be used to sort out some of these issues. For example, there are striking differences between exotic and conventional superconductors in the effect on the infrared response of doping with impurities that limit the scattering time of the quasiparticles. Doped d-wave superconductors do not develop a sharp gap signature at  $\omega = 2\Delta$  as they approach the dirty limit where the scattering rate  $1/\tau > 2\Delta$  as described by Mattis and Bardeen.<sup>18</sup> Instead of a region of perfect reflectance followed by a sharp onset of absorption at  $2\Delta$ , as seen in conventional materials, d-wave materials show a low-frequency Drude-like absorption from defects surrounded by regions of normal material.<sup>19,20</sup> For this test it is necessary to measure the reflectance accurately in the gap region of doped samples in the region of  $\hbar\omega = 2\Delta$ .

It has been suggested<sup>7</sup> that the sensitivity of  $T_c$  to non-magnetic defects in the borocarbides is due to changes in  $N(0)$ , the density of states at the Fermi level, that are related to a peak in the density of states near the Fermi energy  $E_F$  seen in band structure calculations.<sup>12,17</sup> One effect is the valence effect, where, in the rigid band picture, doping with holes or electrons will sweep  $E_F$  across this peak and change  $N(0)$ . Another is where doping with non-magnetic impurities broadens the peak which leads to the reduction of  $N(0)$  which in turn reduces  $T_c$ . One of the advantages of infrared spectroscopy over dc transport measurements is that it allows a separate determination of the scattering rate  $1/\tau$  and the free carrier plasma frequency  $\omega_p$  which is related to  $N(0)$ . Any dramatic changes to the plasma frequency with doping would be seen as a change in the Drude spectral weight with doping. There will also be changes to the slopes of the resistivity curves with temperature which, in accord with Matthiessen's rule, should not change with doping

if it affects the carrier life time but not the density of states.

Infrared spectroscopy can also be used to map out the spectrum of excitations that couple to the electrons. It was shown that BCS superconductors have peaks in the second derivative of the absorption spectrum ( $A = 1 - R$ , where  $R$  is the reflectance)<sup>21,22</sup> at the frequencies of longitudinal and transverse phonons, thus confirming the mechanism of electron-phonon interaction in these materials. For this test one has to be able to measure the second derivative of the reflectance in the region of the relevant excitations. To get the good signal-to-noise ratio necessary for such experiments large single crystals are needed.

Several studies of the optical conductivity of the borocarbides have been published.<sup>23,24,25</sup> Widder *et al.*<sup>23</sup> reported on reflectivity and electron loss spectroscopy on ceramic samples of  $\text{LuNi}_2\text{B}_2\text{C}$  at room temperature for frequencies up to 50 eV. They find an overall metallic response with a plasma frequency of 4.25 eV and an electron-phonon coupling parameter  $\lambda_{tr} = 1.2$ . Bommeli *et al.* measured both  $\text{LuNi}_2\text{B}_2\text{C}$  and  $\text{YNi}_2\text{B}_2\text{C}$  over a wide range of temperatures and frequencies<sup>24</sup> reporting a strong absorption in the pure  $\text{LuNi}_2\text{B}_2\text{C}$  material with an onset of  $100 \text{ cm}^{-1}$ , well below any significant phonon density of states. They also claim to see a dirty limit superconducting gap in the undoped material while, according to transport measurements,<sup>8</sup> the undoped materials should be in the clean limit. In a recent paper Kim *et al.* show measurements at room temperature in  $\text{LuNi}_2\text{B}_2\text{C}$ <sup>25</sup> supplementing infrared reflectance with ellipsometry measurements at higher frequency. They also studied the effect of annealing on their polished samples. They reported a screened plasma frequency of 3.76 eV for an annealed sample and 3.01 eV for an unannealed sample. Both samples were polished. They find a Drude-like frequency-independent scattering rate below 0.3 eV but a gradual rise in scattering above this frequency signaling non-Drude behaviour in the midinfrared.

Cheon *et al.* reported on dc transport in a series of cobalt doped  $\text{LuNi}_2\text{B}_2\text{C}$  single crystals.<sup>8</sup> They found a dc resistivity that was linear in temperature with an intercept on the temperature axis at 35 K at  $T = \theta_D/10$ .<sup>13</sup> The slope of the resistivity increased only slightly with cobalt doping, providing evidence that any changes in the density of states at the Fermi surface with cobalt doping were small. We decided to investigate the issue of the superconducting gap in clean *vs.* dirty samples in the borocarbides using samples from the Ames group, the same source as those used in the Bommeli *et al.* work.

## II. EXPERIMENT

We used flux grown single crystals in this work characterized extensively by dc resistivity and magnetic susceptibility.<sup>8,26</sup> The reflectance measurements were done on natural growth faces normal to the c-axis. To

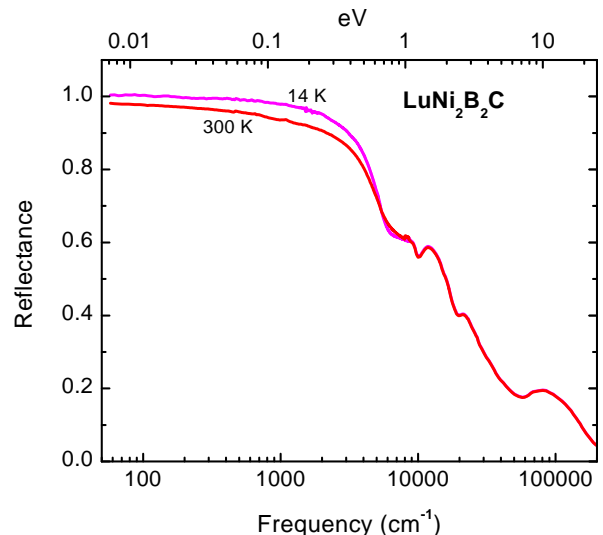


FIG. 1: The reflectance of  $\text{LuNi}_2\text{B}_2\text{C}$  at two temperatures. The data above 5 eV is from Widder *et al.*<sup>23</sup>

correct for irregularities of the surface, which were mainly vertical steps, the sample reflectance was referenced to spectra where the sample was coated with a gold layer, evaporated *in situ*.<sup>28</sup> The as-grown crystals have tiny droplets of  $\text{Ni}_2\text{B}$  on them. The visible ones occupy a small fraction of the surface area and our gold evaporation technique tends to suppress curved surfaces in favour of flat ones. Metallic droplets that are much smaller than the wavelength can give rise to an absorption band in the region of  $\omega_p/\sqrt{3}$ .

Most of the measurements were carried out in a cold-finger flow cryostat with a minimum sample temperature of 10 K. A home made rapid-scan interferometer was used in the far-infrared with He-cooled bolometer detectors below  $700 \text{ cm}^{-1}$  and an MCT detector up to  $8000 \text{ cm}^{-1}$ . High frequency measurements were done with a grating spectrometer, and in the superconducting state, a polarizing interferometer and an immersion dewar with a He-3 bolometer were used between 5 and  $60 \text{ cm}^{-1}$ .

Figure 1 shows the reflectance of a crystal of pure  $\text{LuNi}_2\text{B}_2\text{C}$  over a wide range of frequencies at ambient temperature and at 14 K. Above 5 eV we have merged our data with the EELS data of Widder *et al.*<sup>23</sup> The data showed little temperature dependence at  $8000 \text{ cm}^{-1}$  and we made only room temperature measurements above this frequency. At low frequency the reflectance in the different spectral regions, measured with different spectrometers and detectors, generally agreed to within 0.5 % in the region of overlap, whereas at higher frequencies the mismatch could be as much as several percent.

Figure 2 shows the low frequency region on an expanded scale at three temperatures. The solid lines refer to the pure sample of  $\text{LuNi}_2\text{B}_2\text{C}$  and the dashed curves to the sample with 9 % Co doping. The fine structure on the curves is noise.

A comparison of our measured reflectance with data

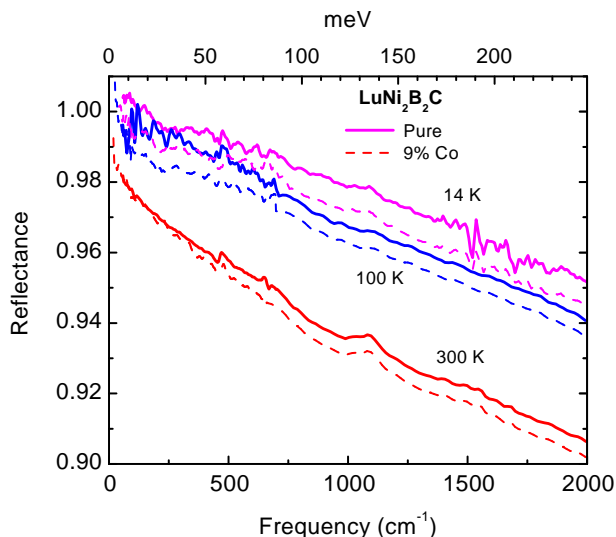


FIG. 2: Low-frequency reflectance of  $\text{LuNi}_2\text{B}_2\text{C}$  at three temperatures. The solid curves are for the undoped sample and the dashed ones for a sample with 9 % cobalt doping. The fine structure is noise.

from other groups shows in general reasonably good agreement with most of the previous work but with some notable discrepancies. First, our reflectances are in general higher than what has been reported by previous investigators. Part of this difference we attribute to our use of as-grown single crystal surfaces since polishing will introduce surface damage leading to additional absorption particularly at higher frequencies. Kim *et al.* find that by annealing the polished crystals a substantial increase in reflectance can be obtained.<sup>25</sup> We have found, in the past, that to obtain good reflectance spectra of metals in the ultraviolet it is necessary to electropolish the samples.<sup>29</sup> The reflectances of our as-grown single crystal surfaces are much higher than the polished samples leading to conductivities in the interband region that are as much as three times higher than those of the polished samples.

At  $800\text{ cm}^{-1}$  at room temperature, we measure a reflectance of 94 % whereas both Kim *et al.* and Bommeli *et al.* report  $\approx 91\%$  in polished samples. We fail to see the strong absorption seen by Bommeli *et al.* at low temperature with an onset at  $50\text{ cm}^{-1}$  where the reflectance falls rapidly from 99 % at  $50$  to 93 % at  $150\text{ cm}^{-1}$ . In all our samples, doped and undoped, the low temperature reflectance below  $700\text{ cm}^{-1}$  was above 98 %, as expected for a good metal.

The overall high reflectance of these single crystals places demands on an accurate calibration of the absolute value of the reflectance. We calibrated our system by using polished stainless steel and a lead indium alloy as primary standards. We started by measuring the dc resistivity of these reference samples and used a Drude model to calculate the absolute value of the reflectance. These calibrations were used to determine the reflectance of our evaporated gold coating which was our secondary stan-

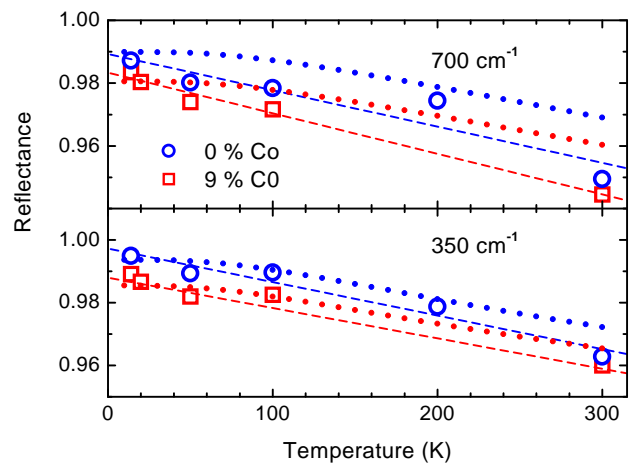


FIG. 3: The temperature dependence of the reflectance at two frequencies. The circles are data for the pure sample, the squares for the cobalt-doped sample. The dashed lines are least squares fits to the experimental points. The small points are for a theoretical model based on the interaction with a mode at  $170\text{ cm}^{-1}$  with parameters fit to dc transport and an assumed plasma frequency of  $3.3\text{ eV}$  (top points pure and bottom doped samples).

dard. Runs were rejected where the reflectance changed by more than 0.5 % between the beginning and the end of the run. As another check we compared our reflectances in the low frequency region with the Drude model based on dc resistivity measurements of crystals prepared in the same way as shown in Fig. 3 and Fig. 4.

Figure 3 gives a picture of the reproducibility of our measurements. We have plotted the reflectance at  $350\text{ cm}^{-1}$  and at  $700\text{ cm}^{-1}$  as a function of temperature for our two samples. In this spectral region  $\omega\tau > 1$  and  $R = 1 - 2/(\omega_p\tau)$ . As the discussion below shows, we find a plasma frequency of  $\omega_p = 3.3\text{ eV}$ . With this value we can relate our reflectance measurements directly to dc resistivity ( $\rho = 4\pi/(\omega_p^2\tau)$ ). The predicted reflectances from the dc resistivity are shown as small symbols in Fig. 3 for the two samples. We see generally excellent agreement in the temperature dependence as well as the difference in the two sample curves due to the doping induced elastic scattering. The dashed curves are a least squares fit of a straight line to the experiments. The root mean square deviation from the straight line is less than 0.15 % for all the curves. However the high frequency curves fall systematically below the dc transport prediction. This is due to the rising  $0.15\text{ eV}$  mid-infrared band that has a threshold in this spectral region.

To obtain the optical conductivity we performed Kramers-Kronig analysis of the reflectance spectra. For this it is necessary to extend the data at low and high frequencies. At low frequencies we assumed a Drude model where the parameters were fit to the lowest measured frequency,  $60\text{ cm}^{-1}$  for the undoped sample and  $20\text{ cm}^{-1}$  for the cobalt doped sample. At high frequency, from  $5\text{ eV}$  to  $35\text{ eV}$ , we used the data of Widder *et al.*<sup>23</sup> and

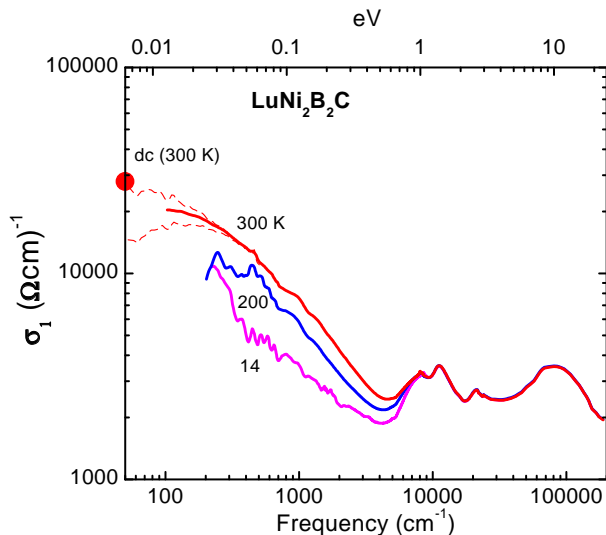


FIG. 4: The optical conductivity of pure  $\text{LuNi}_2\text{B}_2\text{C}$  at three temperatures. The dashed lines show estimated error limits based on a 0.5 % uncertainty of the 100 % line. The circular symbol on the vertical axis is the dc conductivity at room temperature. The decreasing conductivity as the temperature is lowered is due to the narrowing of the Drude peak.

beyond that a power law  $R \propto \omega^{-1.5}$  to  $\omega = 100$  eV and  $R \propto \omega^{-4}$  above 100 eV.

Figure 4 shows the optical conductivity for the undoped sample at 300, 200 and 14 K for the whole measured range. The dashed curves are estimated errors based on a 0.5 % error in the absolute value of reflectance. The solid point is the dc resistivity measurement at room temperature of Cheon *et al.*<sup>8</sup> Our optical data match the dc data within our experimental error. The error of the dc data is  $\pm 10\%$  and mainly due to uncertainties in contact geometry. As the temperature is lowered the conductivity drops in the midinfrared and rises in the far infrared. We are unable to show far infrared conductivities below  $200 \text{ cm}^{-1}$  because the reflectance becomes too high for accurate Kramers-Kronig analysis.

Figure 5 shows the conductivity of the doped sample at two temperatures, along with the pure sample, shown with solid lines. It can be seen clearly that while the doping has little effect at room temperature, at low temperature the Drude peak is broader as expected from the additional scattering.

The measurements with the polarizing spectrometer in the superconducting state for the 9 % doped sample are shown in Fig. 6. To increase the sensitivity we only show a reflectance ratio between the superconducting state and normal state shown as the solid curve in the figure. The dirty limit BCS superconducting gap signature can be seen clearly as a drop in the ratio at  $22 \text{ cm}^{-1}$ . The dashed curve shows the calculated reflectance ratio based on dc conductivity of the 9 % doped sample. We estimate a gap value  $2\Delta = 24 \pm 2 \text{ cm}^{-1}$ .

The disagreement in our data of the peak amplitude

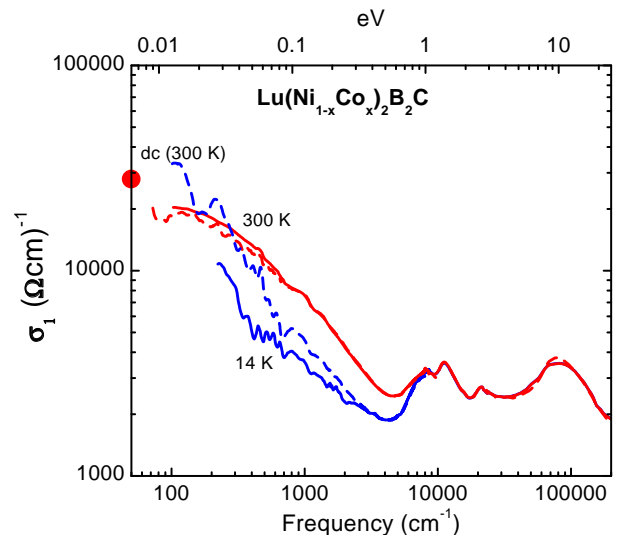


FIG. 5: The conductivity of the 9 % cobalt-doped sample (dashed lines) and the undoped sample, (solid lines). The solid ball on the vertical axis is the dc conductivity. While there is little difference at room temperature, the Drude peak of the doped sample is substantially broader at low temperature.

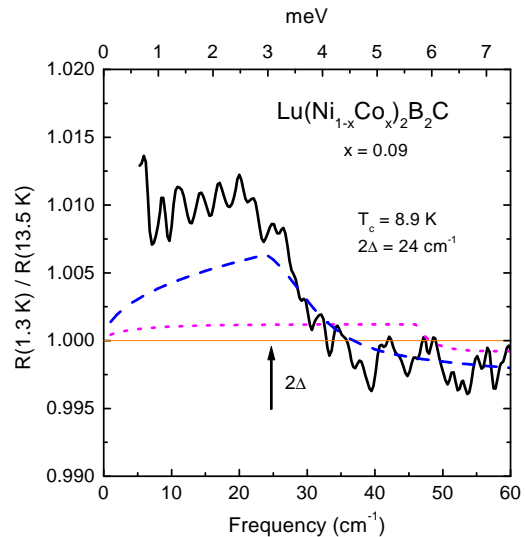


FIG. 6: The reflectance in the superconducting state at 1.3 K divided by the normal state reflectance at 13.5 K. The superconducting gap can be seen as an onset of absorption in the normal state. A BCS theoretical curve for this sample is shown as the curve with the long dashes. The dotted curve is a calculation for the undoped sample. The undoped sample is in the clean limit and the gap signature is predicted to be weak.

in the observed reflectance ratio with a BCS calculation is 0.5 %. This difference is larger than we expect from such a measurement where the sample is not moved and the two measurements are done within minutes of one another. We have measured a lead indium alloy in the same geometry without observing a discrepancy between

the dc transport prediction and the reflectance ratio. The calculation assumes the superconductor to be a perfect reflector in the gap region. Any residual absorption in the superconducting state due to strong gap anisotropy or a second phase on the sample surface would reduce the absorption below the calculated value and have the opposite effect to what we observe. An overall decrease in detector sensitivity with increasing temperature may be partially responsible for the discrepancy but it would have the effect of uniformly shifting the ratio upward causing the data above the gap value to exceed unity. We do not observe such an effect here although we cannot rule out a 0.2 % contribution from this cause. Since we have used dc resistivity to estimate the strength of the normal state absorption any discrepancy between the resistivity of our sample and the bulk measurement could explain the discrepancy. However the agreement at higher frequencies shown in Fig. 3 rules out any large discrepancies.

The model predicts a sharp change of slope at  $2\Delta$  whereas our experiments show what might be two steps, one at 22  $\text{cm}^{-1}$  and another at 26  $\text{cm}^{-1}$ , which may be due to gap anisotropy as proposed by Yang *et al.*<sup>5</sup> based on Raman spectroscopy done in different scattering geometries. However scattering due to the Co dopants would be expected to remove any such anisotropy.

The curve with the long dashes shows the calculated spectrum for the pure sample. The expected gap signature is weak since the sample approaches the clean limit with  $1/\tau = 17 \text{ cm}^{-1}$ , determined from the dc conductivity with  $\omega_p = 3.3 \text{ eV}$  and  $2\Delta = 46 \text{ cm}^{-1}$  from Raman spectroscopy. We measured the pure sample reflectance ratio but failed to see any sign of a superconducting gap in the reflectance ratio of our samples within the estimated noise level of  $\pm 0.002$  in the reflectance ratio.

### III. RESULTS

There are two popular ways of analyzing the conductivity if it does not follow the standard Drude form. The first, the two component method, is to fit the conductivity to a Drude peak centered at zero frequency and add a second component consisting of a set of oscillators in the mid-infrared to allow for any additional non-Drude absorption. The second method, the extended Drude model, introduced by Allen and Mikkelsen,<sup>27</sup> assumes that the Drude form applies throughout the infrared but that the Drude scattering rate increases with frequency, making, in effect, the Drude peak broader as the frequency increases. The first method accounts well for any parallel channels of conductivity such as optic phonons or low-lying interband transitions. The second method is needed when the interaction of the free carriers is strong and a Holstein sideband is formed at low temperatures. At high temperatures this sideband merges with the Drude absorption forming an approximate overall Drude-like band. In the absence of a detailed theory of the optical conductivity both methods have value in

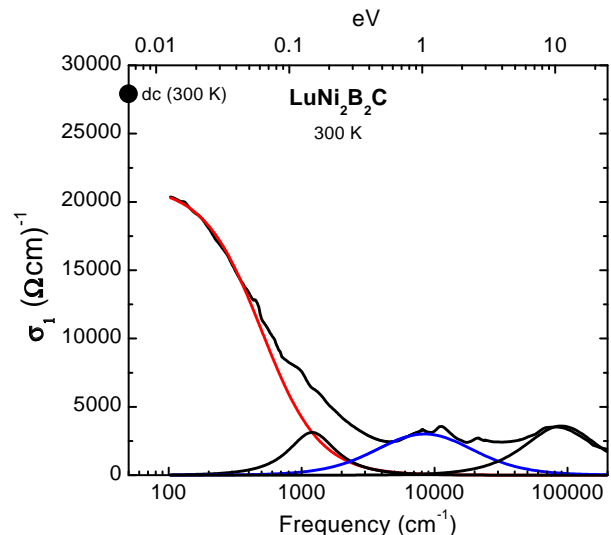


FIG. 7: Oscillator fits to the reflectance (solid curve). In addition to the Drude term at low frequency, three oscillators are needed to describe the conductivity at higher frequencies.

the analysis of the data if one keeps open the possibility that some of the mid-infrared oscillators have no real physical meaning or that the increase in the scattering rate seen in the one-component analysis may be due to interband processes and not to self energy effects on the free carriers.

The two component picture is illustrated in Fig. 7 where we show an oscillator fit to the conductivity for the undoped sample at room temperature. For the undoped sample at 300 K the following oscillators were used, (center frequency, width, and plasma frequency, in  $\text{cm}^{-1}$ ): 0, 500, 25200; 1200, 1200, 15000; 8410, 20000, 60000; 90000, 150000, 180000. It is clear that the simple Drude form does not fit at high frequency and additional Lorentz oscillators are needed to fit the data. The two high frequency oscillators can be identified as due to interband transitions<sup>23</sup> since band structure calculations indicate a gap in the density of states just below the Fermi level rising to a strong peak about 2 eV below the Fermi level. Combining this hole density of states with the sharp peak at the Fermi level would predict an optical conductivity that rises gradually from low frequencies to form the plateau we see in the 1 to 10 eV region. It is difficult, in the absence of a detailed joint density of states, to say if there is a low frequency threshold to the optical conductivity but since the dispersion curves show several band crossings very close to the Fermi level, one cannot rule out an interband conductivity that extends to zero frequency.

The midinfrared oscillator at 0.15 eV is more difficult to assign. Widder *et al.*<sup>23</sup> have assigned the spectral weight in this region to the frequency dependent scattering rate of phonons, but as we will show below, it is difficult to get a consistent picture of the data in this spectral region with a phonon spectrum that is confined

to the known phonon density of states. Fig. 9 (to be discussed below) shows that there is an absorption threshold at  $700 \text{ cm}^{-1}$  at low temperature which suggesting that interband transitions may set in at this frequency. However the onset frequency of the threshold is strongly temperature dependent, moving to  $100 \text{ cm}^{-1}$  at 300 K. This temperature dependence is difficult to explain in terms of a simple Fermi function expected for interband transitions where a broadening of only  $k_B T \approx 200 \text{ cm}^{-1}$  is expected.

The spectral weight under the 0.15 eV oscillator could also be the result of a multiphonon side-band of the Drude peak. From its spectral weight we estimate an additional mass-enhancement factor of 1.35 and a total free carrier plasma frequency of 3.64 as opposed to 3.12 eV if the 0.15 eV oscillator is assigned to interband transitions. A complete Eliashberg calculation would be needed to see if this model will give a consistent picture of the gap ratio, the coupling constant  $\lambda$  and the transition temperature  $T_c$ .

There are several other ways of estimating the Drude weight from our data. The Drude component in Fig. 7 has a plasma frequency of 3.14 eV for the undoped sample. If we scale it to agree with the dc resistivity we get 3.6 eV. Another method uses the temperature dependence of the reflectance shown in Fig. 3 and compares it to the temperature dependence of the dc resistivity. The derivative of the dc resistivity is given by  $d\rho/dT = \frac{4\pi}{\omega_p^2} d\gamma/dT$  where  $\gamma$  is the scattering rate. On the other hand the reflectance in the relaxation region, where  $\gamma < \omega$  is given by  $1 - R = 2\gamma/\omega_p$ , where  $R$  is the reflectance. This equation can be differentiated with respect to  $T$  and the relaxation rate derivative  $d\gamma/dT$  can be eliminated between these two equations to give  $\omega_p = 2\pi(1 - R)'/\rho'$  where the primes denote temperature derivatives. This method is not subject to errors in absolute reflectance as it uses the temperature variation as input. Using this method with the fitted curves in Fig. 3. along with the resistivity data of Cheon *et al.*<sup>8</sup> we obtain an average plasma frequency of  $3.4 \pm 0.15$  eV directly from the reflectance without using data from Kramers-Kronig analysis. As an average of the two methods we adopt the plasma frequency of our pure sample of  $3.3 \pm 0.2$  eV.

Our results are lower than the 4.25 eV value of Widder *et al.* who included the 0.15 eV peak in the Drude spectral weight. Bommeli *et al.* find a two-component low-frequency spectrum with a Drude weight of 0.73 eV and an additional mid infrared band with a total oscillator strength of 4 eV by including the broad absorption at  $500 \text{ cm}^{-1}$ . We have found no evidence for this low frequency component. Kim *et al.* using polished and annealed samples find  $\omega_p = 3.76$  eV for the screened plasma frequency determined from the zero crossing of  $\epsilon_1$ . The zero crossing of  $\epsilon_1$ , obtained from Kramers-Kronig analysis of our reflectance occurs at the same frequency. However to get the unscreened plasma frequency  $\omega_p$  a correction has to be made for the very high frequency dielectric constant

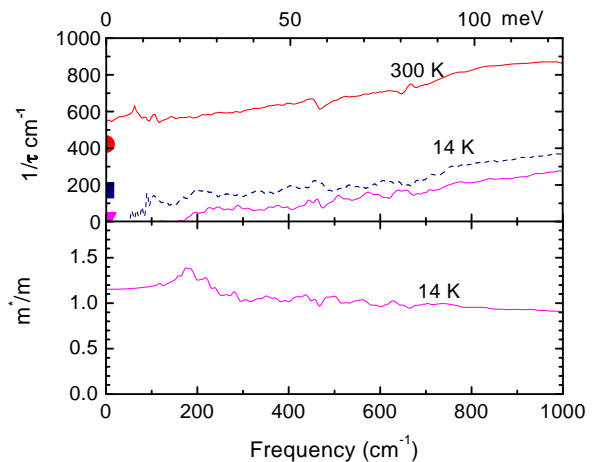


FIG. 8: Frequency dependent scattering rate, top panel, and the effective mass, lower panel, obtained from the extended Drude formula, assuming a plasma frequency of 3.3 eV. The dashed line is for the cobalt-doped sample. The symbols on the axis are dc values of the scattering rate, corresponding to the optical conductivity curves.

which is not known accurately.

The frequency-dependent scattering rate formalism starts with the extended Drude formula:

$$\sigma(\omega, T) = \frac{1}{4\pi} \frac{\omega_p^2}{1/\tau(\omega, T) - i\omega[1 + \lambda_{tr}(\omega, T)]},$$

where  $1/\tau(\omega, T)$  is the frequency dependent scattering rate and  $1 + \lambda_{tr}(\omega, T) = m^*/m$  is the mass renormalization factor. These can be calculated from the real and imaginary parts of the optical conductivity:

$$1/\tau(\omega) = \frac{\omega_p^2}{4\pi} \text{Re}\left(\frac{1}{\sigma(\omega)}\right),$$

and

$$1 + \lambda_{tr}(\omega) = -\frac{\omega_p^2}{4\pi\omega} \text{Im}\left(\frac{1}{\sigma(\omega)}\right).$$

The frequency dependent scattering rate is shown in Fig. 8 along with the mass renormalization. Both are based on an assumed plasma frequency of 3.3 eV for the free carriers and a high frequency dielectric constant of 1.0. The choice of plasma frequency affects the overall scale of the curves. The choice of high frequency dielectric constant has little effect in this frequency region where  $\epsilon_1$  and  $\epsilon_2$  are large. We see a monotonic increase in scattering rate with frequency. The solid curves are for the pure sample and the dashed one for the doped one. The symbols on the vertical axis are the values from the dc conductivity assuming a plasma frequency of 3.3 eV.

The lower panel of Fig. 8 shows  $m^*/m = 1 + \lambda_{tr}$  for the pure sample at low temperature, which is, within a factor of  $\omega$ , the imaginary part of  $1/\tau$ . One can read off the calculated electron-phonon coupling constant for dc transport, the zero-frequency value,  $\lambda_{tr}(0)$  to be 0.15. The

value obtained more directly from dc transport is 0.34, based on a plasma frequency of 3.3 eV and the assumption that the transport curves have reached their high frequency linear limit at 300 K when  $1/\tau = 2\pi k_B T$ . A strong contribution from high frequency phonons would raise the dc value of  $d\rho/dT$  and lead to an even larger  $\lambda_{tr}$ . We do not feel that discrepancy between the transport value and the optical value is significant since the curves in Fig. 7 have large uncertainties due to the high reflectance of the undoped sample at low frequencies.

It is important to stress the difference between the curves in Fig. 8 and the corresponding data for the cuprates.<sup>30</sup> First, the overall scale of scattering in the cuprates is an order of magnitude higher to the point where the scattering rate is larger than the frequency, leading to a breakdown of Fermi liquid theory which assumes that  $1/\tau \ll \omega$ . Second, while the variation of scattering is linear with frequency in both materials, in the cuprates the curves extrapolate back to a finite positive intercept on the  $1/\tau$  axis that scales as  $T$  and goes to zero at  $T = 0$ . This is characteristic of quantum fluctuations.<sup>31</sup> For the borocarbides the intercept at

$T = 0$  is on the negative  $1/\tau$  side resulting in a finite intercept on the frequency axis, which is of the order of the Debye frequency, as expected for a Bloch-Grüneisen conductivity. The Debye frequency of LuNi<sub>2</sub>B<sub>2</sub>C is 250 cm<sup>-1</sup> from a Debye temperature of 360 K measured by neutron spectroscopy<sup>15</sup> in good agreement with the point of intersection of the low temperature reflectance curve with the  $R = 1$  axis.

A fit of a theoretical model directly to the reflectivity avoids the propagation of errors associated with Kramers-Kronig analysis and the extraction of the parameters of the extended Drude model. This is particularly relevant in a good metallic system where the reflectivity is close to unity. The procedure is to start with a model  $\alpha_{tr}^2(\Omega)F(\Omega)$  of the electron phonon spectral function<sup>16,33</sup> weighted by the amplitude for large angle scattering and then calculate the optical properties and compare them to experiments.

To calculate the reflectance spectra we use the extended Drude formalism with the scattering rate given by Shulga et al.<sup>33</sup>:

$$\frac{1}{\tau}(\omega, T) = \frac{\pi}{\omega} \int_0^\infty d\Omega \alpha_{tr}^2(\Omega) F(\Omega) \left[ 2\omega \coth\left(\frac{\Omega}{2T}\right) - (\omega + \Omega) \coth\left(\frac{\omega + \Omega}{2T}\right) + (\omega - \Omega) \coth\left(\frac{\omega - \Omega}{2T}\right) \right],$$

where  $T$  is the temperature, measured in frequency units. Following Gonnelli *et al.*<sup>10</sup> we place a restriction on the spectral functions demanding that they fit the slope and absolute magnitude of the dc resistivity of LuNi<sub>2</sub>B<sub>2</sub>C. We use a plasma frequency of 3.3 eV in our models.

The simplest model is a single Einstein oscillator. We find that an oscillator at 170 cm<sup>-1</sup> with  $\lambda_{tr} = 0.33$  gives a fairly good value of the room temperature resistivity and the temperature derivative of the resistivity (35  $\mu\Omega\text{cm}$  and 0.135  $\mu\Omega\text{cm/K}$ , vs. the experimental values of 36  $\mu\Omega\text{cm}$  and 0.127  $\mu\Omega\text{cm/K}$ ). The bold curves in Fig. 9 are the calculated spectra based on this model.

Another model uses the phonon density of states as determined by neutron scattering. The bare spectrum gives a rather poor fit to the dc transport and Gonnelli *et al.* found that they had to enhance the low frequency modes (below 38 meV) by 0.7 and the high frequency ones by 0.25, a ratio of 2.8 in the enhancement of the low frequency spectrum. They used a  $\lambda_{tr}$  of 0.53 based on a plasma frequency of 4.25 from the Widder *et al.*<sup>23</sup> optical measurements.

Because we find a lower plasma frequency of 3.3 eV we find that somewhat different parameters than those used by Gonnelli *et al.* are necessary to fit the resistivity. Taking the Gonnelli spectrum as a reference, we have multiplied the low frequency part by 0.23, the upper band above 38 meV by 0.48, a ratio of 2.1 in the enhance-

ment of the low frequency spectrum. These parameters were adjusted to give reasonable agreement with the temperature dependence of the dc resistivity. The resulting spectrum is similar to what is shown for the Einstein oscillator in Fig. 9.

The fit of both models to our reflectance is good at low frequency and well within experimental uncertainties, but there are serious deviations at high frequency which become more marked with increasing temperature. These deviations exceed our experimental uncertainty.

It is not possible to remove the high frequency discrepancy by manipulating the coupling to the various phonon frequencies. To obtain the strong scattering seen at high frequencies it is necessary to add oscillators above the phonon spectrum with a continuous distribution of frequencies, a spectrum of the Marginal Fermi liquid type as seen in the cuprate superconductors.<sup>31</sup> However such a model cannot be justified in this case since the scattering rate curves shown in Fig. 8 intersect above unity, signifying the coupling to finite frequency bosons and not to quantum critical fluctuations where the intercept occurs at unit reflectance at low temperature.<sup>31</sup>

We think a more likely scenario is one where the threshold of absorption seen in Fig. 8 is a manifestation of the onset of either multi-phonon processes or interband transitions as shown by the 0.15 eV band in the conductivity spectra, the same phenomenon that was responsible for

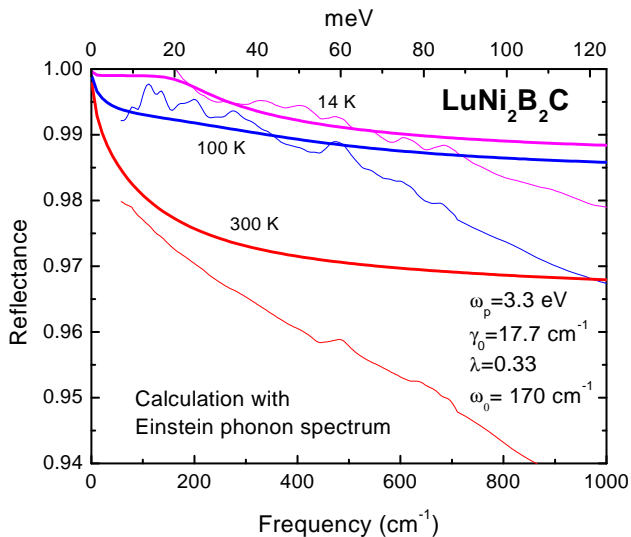


FIG. 9: Calculated reflectance based on the electron-phonon interaction with a coupling constant  $\lambda_{tr}$  obtained from the dc resistivity assuming an Einstein spectrum of a single phonon at  $170 \text{ cm}^{-1}$ . The agreement with the measured reflectance (thin curves) is good at low frequency but strong additional absorption sets in at  $700 \text{ cm}^{-1}$  at 14 K

the mid-infrared oscillator shown in Fig. 7. There is also the possibility of a contribution to the mid-infrared absorption by the  $\text{Ni}_2\text{B}$  droplets.

#### IV. DISCUSSION

We first address the question of the plasma frequency and its variation with doping. Based on several methods of analysis we find a Drude weight at room temperature of  $3.3 \text{ eV}$  for the undoped sample. Other investigators have reported somewhat higher values as a result of the inclusion of some midinfrared spectral weight in the Drude peak giving a value closer to  $4.25 \text{ eV}$ .<sup>23,24</sup> Pickett and Singh<sup>12</sup> calculate a plasma frequency from band structure to be  $5.1 \text{ eV}$ . However Michor *et al.*<sup>13</sup> suggest, from an analysis of specific heat data, that this is an over estimate.

The question of the doping dependence of the Drude weight is more difficult. It is clear from most of our measurements that the changes in the spectra with Co doping are relatively slight and the methods used in the previous paragraphs are subject to errors of the order of 10% and not accurate enough for this task. To help reduce systematic errors we use the integrated spectral weight as a measure of Drude weight. Fig. 10 shows the quantity  $N_{eff}$  which is the number of electrons contributing to the conductivity in the unit cell of volume  $V_{cell}$ :

$$N_{eff}(\omega) = \frac{2mV_{cell}}{\pi e^2} \int_0^\omega \sigma(\omega') d\omega'$$

We show  $N_{eff}$  at room temperature, for the pure sample,

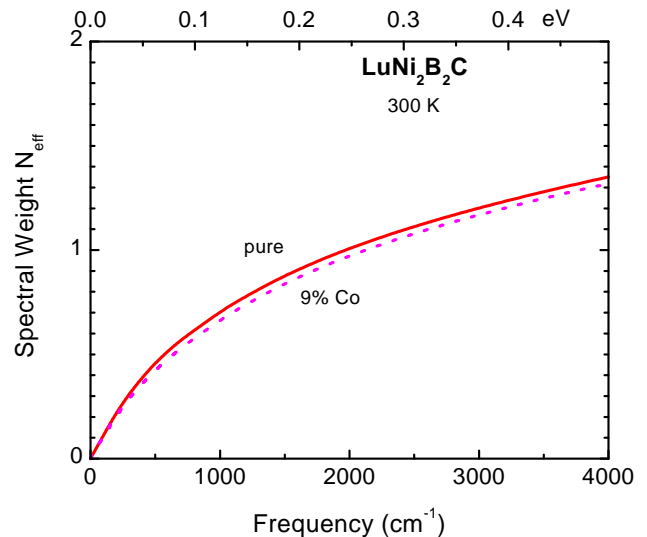


FIG. 10: Partial conductivity sum rule for the pure and the doped samples. The small enhancement of conductivity in the pure sample would imply a small enhancement of the density of states at the Fermi surface. The small difference is not significant within our margin of error.

solid curve, and the 9 % doped sample, dashed curve. The pure curve is higher by about 7 % in the region of the Drude peak. This difference is not significant in view of our error of 0.5 % in reflectance which propagates to give an uncertainty of 7 % for the spectral weight. The density of states at the Fermi surface is proportional to the square of the plasma frequency and appears to be reduced by 7 % by the cobalt doping if we believe the difference data of Fig. 10. The overall spectral weight reaches one electron per unit cell at the frequency where the interband contribution takes over from the Drude conductivity.

We can compare our change in Drude spectral weight with cobalt doping with what might be expected from the dc resistivity. From the data of Cheon *et al.*<sup>8</sup> the slope of the resistivity changes from  $0.127$  to  $0.140 \mu\Omega\text{cm/K}$  in going from the pure sample to the 9 % cobalt doped one. If this effect is from the change in the Drude plasma frequency it would correspond to a change in  $\omega_p^2$  of 10 %, somewhat higher than the 7 % that we get from the change in the infrared Drude weight. However the dc measurements are subject to an error of  $\pm 10 \%$  due to uncertainties in contact geometry and the difference is not significant. It should be noted that the dc resistivity slope is also proportional to the coupling constant  $\lambda_{tr}$  which could change with doping. It appears that neither method, the infrared or the dc transport is able to put an accurate limit on the change in Drude weight with cobalt doping. All that can be said is that it appears to be less than 10 % from both measurements.

Our value of  $2\Delta/k_B T_c = 3.9 \pm 0.4$  for the doped sample places it in the regime of weak to moderately strong coupling superconductivity. Raman scattering on



a pure sample of this material gives a strong coupling gap ratio of 4.1,<sup>6</sup> as do thermodynamic data, such as the magnitude of the specific heat jump.<sup>13</sup> However, tunneling spectroscopy point to a weak coupling value of the ratio.<sup>34</sup> A weak coupling value of the gap parameter is also consistent with our electron phonon coupling parameter  $\lambda_{tr} = 0.33$ .<sup>35</sup>

In summary, we have presented reflectance data on as-grown surfaces of  $\text{LuNi}_2\text{B}_2\text{C}$  which differ in several aspects from those measured by previous investigators along with an analysis based on free electron theory. First our measurements confirm that on the whole this material has the electrodynamic properties of a good metal. We are able to fit the reflectance data at low frequency to models of electron phonon interaction with parameters derived from dc transport on crystals from the same source. At higher frequency additional absorption is observed which we attribute to multi-phonon processes or interband transitions. We find a Drude plasma frequency of 3.3 eV and an electron-phonon coupling constant  $\lambda_{tr} = 0.33$ . This low value of  $\lambda_{tr}$  is consistent with our superconducting gap ratio of  $2\Delta/k_B T_c = 3.9$  which we measure from reflectance in the superconducting state in the cobalt doped sample which is in the dirty limit. We do not see any change to the plasma frequency with cobalt doping to a level of  $\pm 10\%$  but do observe an amount of increased scattering which is consistent with Mattheissen's rule.

There remain several open questions. First, what is

the nature of the mid-infrared absorption band at 0.15 eV? Unlike the cuprates where a large portion of the absorption is associated with a Marginal Fermi Liquid spectrum of electronic coupling to the charge carriers with an intercept at zero frequency, the intercept here is Bloch-Grüneisen-like at finite frequency. Second, the accuracy of our experiments was insufficient to yield the detail in scattering rate spectrum necessary to reveal the phonon spectrum. With more accurate infrared data the  $\alpha^2 F(\Omega)$  spectrum of the electron phonon interaction can be mapped out as was done for lead.<sup>22</sup> Also, it would be important to make accurate resistivity measurements at high temperature to look for evidence of coupling to high frequency modes. To see evidence for phonon effects by infrared spectroscopy, the current single bounce reflection measurements do not have enough resolution. Cavity measurements on large enough single crystals at low temperature and high frequency may have enough sensitivity for this. Also, a detailed strong coupling calculation may be able to throw light on the possibility that the 0.15 eV band may be due to strong coupling multi phonon processes.

The work at McMaster University was supported by the Canadian National Science and Engineering Research Council. The Ames Laboratory is operated for the U.S. Department of Energy by Iowa State University under Contract No. W-7405-Eng-82. We would like to thank J.P. Carbotte, Hanhee Paik, and E. Schachinger for valuable discussions.

- 
- \* Present address: II. Physikalisches Institut, Universität zu Köln, 50937 Köln, Germany
- † Present address: National Institute of Chemical Physics and Biophysics, 12618 Tallinn, Estonia
- ‡ Present address: Institute of General Physics, Russian Academy of Sciences, 119991, Moscow, Russia
- § The Canadian Institute of Advanced Research; Electronic address: timusk@mcmaster.ca
- <sup>1</sup> P.C. Canfield, P.L. Gammel, and D.J. Bishop, *Physics Today*, p. 40 (1998).
- <sup>2</sup> G. Wang and K. Maki, *Phys. Rev. B* **58**, 6493 (1998).
- <sup>3</sup> K. Izawa, A. Shibata, Yuji Matsuda, Y. Kato, H. Takeya, K. Hirata, C.J. van der Beek, and M. Konczykowski, *Phys. Rev. Lett.* **86**, 1327 (2001).
- <sup>4</sup> S. Manalo, H. Michor, M. El-Hagary, G. Hilscher, and E. Schachinger, *Phys. Rev. B* **B63**, 104508 (2001).
- <sup>5</sup> In-Sang Yang, M.V. Klein, S.L. Cooper, P.C. Canfield, B.K. Cho, and Sung-Ik Lee, *Phys. Rev.* **B62**, 1291 (2000).
- <sup>6</sup> In-Sang Yang, M.V. Klein, T.P. Devereaux, I.R. Fisher, and P.C. Canfield, *cond-mat/9912492*.
- <sup>7</sup> H. Schmidt, M. Müller, and H.F. Braun, *Physica C* **235**, 779 (1994).
- <sup>8</sup> K.O. Cheon, I.R. Fisher, V.G. Kogan, P.C. Canfield, P. Miranović, and P.L. Gammel, *Phys. Rev. B* **58**, 6463 (1998).
- <sup>9</sup> S.V. Shulga, S.-L. Drechsler, G. Fuchs, K.-H. Müller, K. Winzer, M. Heinecke, and K. Krug, *Phys. Rev. Lett.* **80**, 1730 (1998).
- <sup>10</sup> R.S. Gonnelli, A. Moreno, G.A. Ummarino, V.A. Stepanov, G. Behr, G. Graw, S.V. Shulga, and S.-L. Drechsler, *cond-mat/0007033*.
- <sup>11</sup> H. Suderow, P. Martinez-Samper, S. Viera, N. Luchier, J.P. Brison, and P. Canfield, *Int. Journal of Modern Physics B* **14**, 2840 (2000). *cond-mat/0102152*.
- <sup>12</sup> W.E. Pickett and D.J. Singh, *Phys. Rev. Lett.* **72**, 3702 (1994).
- <sup>13</sup> H. Michor, T. Holubar, C. Dusek, and G. Hilscher, *Phys. Rev. B* **52**, 16165 (1995).
- <sup>14</sup> S.V. Shulga, S.L. Drechsler, G. Fuchs, K.-H. Müller, K. Winzer, M. Heinecke, and K. Krug *Phys. Rev. Lett.* **80**, 1730, (1998).
- <sup>15</sup> F. Gompf, W. Reichardt, H. Schober, B. Renker, and M. Buchgeister, *Phys. Rev. B* **55**, 9058 (1997) .
- <sup>16</sup> P.B. Allen, *Phys. Rev. B* **3**, 305 (1971).
- <sup>17</sup> L.F. Mattheiss, *Phys. Rev. B* **49**, 13279 (1994).
- <sup>18</sup> D.C. Mattis and J. Bardeen, *Phys. Rev.* **111**, 412 (1958).
- <sup>19</sup> D.N. Basov, B.Dabrowski, and T. Timusk, *Phys. Rev. Letters* **81**, 2132 (1998).
- <sup>20</sup> E. Schachinger and J.P. Carbotte, *cond-mat/0105459*.
- <sup>21</sup> R.R. Joyce and P.L. Richards, *Phys. Rev. Lett.* **24**, 1007 (1970).
- <sup>22</sup> B. Farnworth and T. Timusk, *Phys. Rev. B* **14**, 5119 (1976).
- <sup>23</sup> K. Widder, D. Berner, A. Zibold, H.P. Gesserich, M. Knupfer, M. Kielwein, M. Buchgeister, and J. Fink, *Europhysics Lett.* **30**, 55 (1995).
- <sup>24</sup> F. Bommeli, L. Degiorgi, P. Wachter, B.K. Cho, P.C. Canfield, R. Chau, and M.B. Maple, *Phys. Rev. Lett.* **78**, 547

- (1997).
- <sup>25</sup> J.H. Kim, H. Paik, M.-O. Mun, B.K. Cho, S.J. Youn, H.B. Kim, and S.-I. Lee, *Physica C* **341-348**, 2233 (2000).
- <sup>26</sup> B.K. Cho, P.C. Canfield, L.L. Miller, D.C. Johnston, W.P. Beyermann and A.Yatskar, *Phys. Rev. B* **52**, 3684 (1995).
- <sup>27</sup> J.W. Allen and J.C. Mikkelsen, *Phys. Rev. B* **15**, 2952 (1977).
- <sup>28</sup> C.C. Homes, M.A. Reedyk, D.A. Crandles, and T. Timusk, *Applied Optics* **32**, 2976 (1993).
- <sup>29</sup> H.R. Philipp and E.A. Taft, *Phys. Rev.* **121**, 1100 (1961).
- <sup>30</sup> A.V. Puchkov, D.N. Basov, and T. Timusk, *J. Physics; Condensed Matter* **8**, 10049, (1996).
- <sup>31</sup> C.M. Varma, P.B. Littlewood, S. Schmitt-Rink, E.Abrahams, and A.E. Ruckenstein, *Phys. Rev. Lett.* **63**, 1996 (1989).
- <sup>32</sup> S. Manolo and E. Schachinger, cond-mat/0101419.
- <sup>33</sup> S.V. Shulga, O.V. Dolgov, and E.G. Maksimov, *Physica C* **178**, 266 (1991).
- <sup>34</sup> T. Ekino, H. Fujii, M. Kosugi, Y. Zenitani, and J. Akimitsu, *Phys. Rev. B* **53**, 5640 (1996).
- <sup>35</sup> J.C. Carbotte, *Rev. Mod. Phys.* **62**, 1027 (1990).